Single-Crystalline $InVO_4$ Nanotubes by Self-Template-Directed Fabrication

Xi Yi and Jianlin Li[†]

School of Materials Science and Engineering, Shanghai University, Shanghai 201800, China

Zhong Chen and Alfred Tok

School of Materials Science and Engineering, Nanyang Technological University, Singapore 630939, Singapore

[†]*Author to whom correspondence should be addressed. e-mail: jlli@shu.edu.cn*

Single-crystalline $InVO_4$ nanotubes have been successfully synthesized by annealing electrospun precursor fibers. The products were characterized by X-ray diffraction, transmission electron microscopy, and high-resolution transmission electron microscopy, which demonstrated that they are single-crystalline nanotubes. The growth of these nanotubes is considered to be a two-step process involving a self-template-directed mechanism.

I. Introduction

Carbon nanotubes have been a focus in materials research since their discovery in 1991.[1] More recently, noncarbonic nanotubes have also been attracting considerable attention due to their unique properties. Among them, oxide nanotubes (ONTs) are of special interest because of their potential applications in sensors,[2] catalyzers,[3] and microelectronics and nano-scale devices.[4,5] Numerous ONTs have been produced by either template-directed or templateless routes. The former uses physical or chemical

media as templates to guide the growth of ONTs. The templates used include nanofibers,[6] nanotubes,[7] porous aluminum oxides,[8] gelators, and so on.[9,10] However, template-assisted methods have achieved far less in terms of the formation of single-crystalline nanotubes, and choosing the right templates is tedious. The latter, on the other hand, refers to the spontaneous formation of ONTs, for instance, by hydrothermal treatment or calcinations of ceramic powders or films,[11,12] an electrochemical anodizing process,[13] and many other methods.[14,15]

A facile and mass productive approach is yet to be developed for the study and practical applications of ONTs. This paper reports the preparation of single-crystalline $InVO_4$ nanotubes by annealing electrospun precursor fibers, demonstrating a self-template-directed mechanism. Currently, oxide fibers are prepared by calcining precursor electrospun fibers, which are usually a mixture of organic binders and ceramic powders, or a sol thickened with polymer binders.[16,17] Generally, solid or hollow fibers are obtained when a single nozzle or a compound coaxial nozzle is used, respectively.[18] These fibers usually have a diameter of tens of nanometers to micrometers. Annealing of the electrospun precursor fibers used to create solid or hollow multicrystalline nanofibers, the topic of this paper, therefore, represents an important and explored field.

In a previous study,[19] nanotube arrays of $InVO_4$ were prepared by filling the sol into pores of polycarbonate membranes and pyrolyzing through sintering. The tubes produced are multicrystalline and have a diameter of around 100 nm. As a complicated template is needed, it is difficult to obtain nanotubes with further decreased diameters.

To our knowledge, single-crystal nanotubes of $InVO_4$ have not been reported before, and no single-crystal nanotubes have been produced by annealing electrospun precursor fibers.

II. Experimental Procedure

In our experiment, $In(NO_3)_3 \cdot 4.5H_2O$ and NH_4VO_3 with a purity of 99.9% were obtained from the Sinopharm Chemical Reagent Co. Ltd. (Shanghai, China). Poly(vinyl pyrrolidone) (PVP, M_w = 1 300 000) and ethanol of analytical grade were purchased from

Shanghai Chemical Reagent Co. Ltd. (Shanghai, China). All the reagents in this experiment were used as received without any further treatment.

In order to prepare an appropriate solution for electrospinning, 2.55 g $In(NO_3)_3 \cdot 4.5H_2O$ was dissolved in 25 mL acetylacetone and refluxed at 83°C for 2 h to obtain a homogeneous and stable solution A. 0.78 g NH_4VO_3 was dissolved in 25 mL acetylacetone and refluxed at 83°C for 2 h to obtain a homogeneous and stable solution B. Solutions A and B and 17 mL ethanol were mixed and refluxed at 83°C for 2 h to obtain a stable $InVO_4$ solution C. Then, 2.23 g PVP was further added to solution C and refluxed at 80°C for 2 h to obtain the precursor liquid for electrospinning. PVP was used as a binder to enhance the viscosity of the solution.

During electrospinning, the feeding rate of the solution from the syringe was maintained at 0.2 mL/h using a syringe pump. The voltage applied to the needle of the nozzle was 5.6 kV and the distance between the tip of the needle and the stainless-steel grid collector was 7 cm. The fibers produced were peeled off from the collector and dried in air at 80°C for 10 min, and then placed in crucibles and heated in air to 500° and 600°C, respectively, at a ramping rate of 2°C/min. Without the holding time, the fired fibers were then cooled with the furnace. In a control experiment, 20 g of precursor solution was subjected to the same treatment as the electrospun fibers received.

The phase and crystallinity of the specimens were checked using powder X-ray diffraction (XRD, Model D-max II, Danvers, MA) (Cu$K\alpha$ radiation: k = 0.154 nm) at a scanning rate of 0.02°/s in 2θ ranging from 10° to 60°. Transmission electron spectroscopy (TEM), high-resolution transmission electron spectroscopy (HRTEM), and selected-area electron diffraction (SAED) were used to characterize the structures of products on the TEM (Model H800, Hitachi, Ibaraki, Japan) operated at a voltage of 200 kV. Energy-dispersive spectroscopy (EDS, Oxford Inc., Abingdon, UK) was also used to analyze the elemental composition of the as-prepared nanotubes.

III. Result and Discussion

Figures 1(a) and (b) show TEM images showing the dried electrospun fibers, in which darker nanoparticles with an average size of 2 nm can be observed. According to previous works by Xu *et al.*[20] and Touboul *et al.*,[21] these nanoparticles are amorphous $InVO_4$, which is also demonstrated by SAED (inset in Fig. 1(b)). When heated up to 500°C in air, PVP and other organic components would be removed completely, leaving only inorganic components, as Alves *et al.*[22] reported. Meanwhile, electrospun fibers were likely to fracture into segments of $InVO_4$ nanoparticles as a ceramic green body sometimes does when the binder is lost. When heated further to 600°C, the $InVO_4$ nanoparticles were found to crystallize into nanotubes (Figs. 1(c) and (d)). That is, the segments of $InVO_4$ nanoparticles developed into $InVO_4$ nanotubes. The SAED (inset in Fig. 1(c), from several nanotubes rather than a single one), further supports our above-mentioned argument that well-crystallized $InVO_4$ nanotubes are obtained as the product. Because of the shrinkage caused by degradation of PVP and the subsequent sintering, the average diameter of the as-prepared $InVO_4$ nanotubes is much smaller than that of the dried electrospun fibers. In a control experiment, clusters of nanoparticles (Figs. 1(e) and (f)) were derived from directly annealing the precursor sol. Obviously, the electrospinning led to different structures, although they were from the same precursor sol and had undergone the same treatment.

Figure 2(a) presents the XRD pattern of the as-prepared nanotubes (upper) and the nanoparticles from the same precursor sol (lower). The sharp peaks in the XRD patterns show good crystallization of the $InVO_4$ nanoparticles and nanotubes. Comparing them with the $InVO_4$ patterns documented in the powder diffraction files of the JCPDS, both the $InVO_4$ nanoparticles and the $InVO_4$ nanotubes (Fig. 2(a)) prepared in the present work had a monoclinic structure (JCPDS 38-1135, $C2/m$ with a = 10.271 Å , b = 9.403 Å , and c = 7.038 Å). This is in agreement with the result that Xu *et al.*[20] reported. In their work, monoclinic-phase $InVO_4$ was obtained at low temperatures below 700°C. As shown in Fig. 2(a), the only difference in these two patterns was that the peak of plane (002) from the $InVO_4$ nanotubes is stronger than from nanoparticles. The EDS spectrum of the $InVO_4$ nanotubes (Fig. 2(b)) indicated that only oxygen, indium, and vanadium

elements existed in the nanotubes, confirming undoubtedly that the products shown in Figs. 1(c) and (d) are $InVO_4$ nanotubes.

Further examinations (Figs. 3(a) and (b)) of the tube structure showed that these nanotubes had a nearly uniform diameter of 15 nm. The cylindrical walls shown in Fig. 3(a) have a spacing of 0.345 nm, indicating that they are (002) planes. The observation of the HRTEM images shows the appearance of a strong (002) peak in the XRD pattern of Fig. 2(a) (upper one).

It is important to understand how a nanofiber transforms into a nanotube and how the hollow channel of a nanotube is formed. It is obvious that under external thermal annealing, $InVO_4$ nanoparticles inside the nanofibers would, with the removal of organic components, exhibit a sintering tendency and form more dense structures, along with structural crystallization. Recently, Du *et al*.[23] detailed the transformation of the particle-wire-tube for a carbon nanotube, which may shed some light on our current work. As discussed in their paper, Du *et al*.[23] suggested that the essential point is to produce a rigid outer shell before the formation of carbon nanotubes. A similar process has been found in this research (Fig. 4). This mechanism includes three key steps: (a) removing the organic polymer from electrospun fibers by thermal decomposition; (b) self-assembling the oxide nanoparticles into oxide nanowires; and (c) emptying the oxide nanowires into oxide tubular structures. Specifically, in this work, $InVO_4$ nanoparticles formed nanofibers (nanowires) after the organic components were removed. We believed that the driving force for the nanofiber–nanotube transformation lies in the strong tendency of sintering to minimize the surface energy. Because of the confinement by surrounding nanoparticles inside the nanofiber undergoing baking, sintering of the nanoparticles of the nanofiber, usually accompanied by shape change and movement, most likely starts at the outer surface and leaves behind an immobile cylindrical shell around the baked nanofiber. As a result, additional shells formed from a subsequent sintering of the inner particles would predictably attach to the inner surfaces of the initially formed shell, leading to an epitaxial multilayered structure. Under proper conditions, during the sintering, the inner space is left behind within the baked nanofiber through unification of the inherent inner cavities and interspaces of the nanoparticles. After this process, hollow nanotubes are

produced. In other words, a novel method to prepare ONTs, that is, self-template-directed fabrication, is demonstrated in this work.

The above idea is evidenced by the careful observation of a nearly mature nanotube (arrowed in Fig. 3(a)). The tube has an obvious, continuous yet undeveloped ektexine, supporting our explanation that the crystallization takes place first from the outer surface of the nanofiber undergoing baking. A relatively rough outer surface of these nanotubes also confirmed the above explanation. Because when the outermost layer was formed there were no other shells to guide its growth direction. Usually, crystal planes of the lower surface energy are more likely to form the outer surface. The formation of single-crystalline nanotubes, therefore, is a result of preferential growth of crystal planes, in this work, (002) planes. The channel within the tube shown in Fig. 3(a) is still partly filled with agglomerates of nanoparticles to grow into inner layers. Moreover, the spacing of the (002) plane of the tubes is 0.345 nm, slightly greater than that of perfect $InVO_4$ grains, showing that the "loose" (002) planes are piled up layer by layer. One more testimony emerges from the HRTEM images showing the tips of the nanotubes. When the nanotubes were grown from nanofiber segments having flat ends, these tubes usually had round and well-crystallized tips (lower left corner in Fig. 3(a)). When tubes were growing from segments with sharp ends, as shown in Fig. 3(b) (arrowed), the inner layers near the tube tip were gradually and slowly approaching the outer layers under the guidance of the outer shell.

Here one question arises: in previous researches, why did hollow or solid electrospun fibers, when fired, transform into hollow or solid fibers rather than single-crystalline nanotubes. The basic difference lies in the structures of these annealed fibers. For the common baked hollow electrospun fibers, there are two free surfaces: inner and outer surfaces due to their hollow structure and considerable wall thickness. Such a structure allows crystallization or sintering to take place simultaneously on both the surfaces, leading to a multicrystalline wall. Such "double sintering" is assumed to the formation of take place in Wang and Cao's work,[19] where $InVO_4$ nanocrystals attached to the wall of the pores are sintered to form multicrystalline tubes. In this work, by contrast, crystallization takes place only from the outer surface. A rigid crust is thus formed, which

acts as a template for the inner amorphous nanosized particles to grow on, resulting in a single-crystalline tube.

Another key factor is the tiny size (1.5–2) nm of the nano-particles inside the nanofiber. It is well established that smaller particles show a higher tendency toward sintering to minimize the surface energy. Moreover, as the sintering of particles of a tiny size is usually associated with only slight shape changes and movements, such a size ensures the sintering of nanoparticles on the outer surface to form a shell before the coarseness of their counterpart inside the fiber. By contrast, products derived from thermal decomposition tend to be coarser particles, and the sintering of these particles is accompanied by significant shape changes and movements, which makes the formation of an outer shell difficult and leads to the appearance of a solid nanofiber as a result of simultaneous sintering across the whole fiber section. This also explains why ZnO nanofibers instead of tubes were produced in Liu *et al.*'s work, where $Zn(Ac)_2$ was used as the precursor.[24] Further, when ceramic powders are used as a component in the electrospun fibers, the greater size of these particles makes it impossible to produce a hard shell enveloping the baked fiber without the sintering of inside particles.[25]

Last but not the least, the freshly produced $InVO_4$ nanoparticles are amorphous, which means that they are more likely to be restructured than well-crystalline particles. This may be helpful in the formation of the nanotubes.

In the present work, the as-fabricated nanotubes had a diameter of 18 nm. Obviously, the nanotube diameter is closely related to the fiber size and composition. Studies focusing on tuning of the diameter of the nanotubes by varying the size and the composition of electrospun fibers are ongoing, and the results will be reported in a future paper.

IV. Conclusion

Single-crystalline $InVO_4$ nanotubes have been successfully prepared by annealing electrospun precursor fibers. The growth of these tubes is considered to be a two-step process involving a self-template-directed mechanism, during which an outer shell is

formed first, followed by anchoring and epitaxial growth of $InVO_4$ nanoparticles onto the shell. The reported approach may pave the way for the massive production of single-crystalline ONTs.

References

[1]S. Iijima, "Helical Microtubules of Graphitic Carbon," *Nature*, **354**, 56–8 (1991).

[2]J. M. Perez-Blanco and G. D. Barber, "Ambient Atmosphere Bonding of Titanium Foil to a Transparent Conductive Oxide and Anodic Growth of Titanium Dioxide Nanotubes," *Sol. Energ. Mater. Sol. C*, **92**, 997–1002 (2008).

[3]A. B. F. Martinson, J. W. Elam, J. T. Hupp, and M. J. Pellin, "ZnO Nanotube Based Dye-Sensitized Solar Cells," *Nano Lett.*, **7** [8] 21837 (2007).

[4]F. Fabregat-Santiago, E. M. Barea, J. Bisquert, G. K. Mor, K. Shankar, and C. A. Grimes, "High Carrier Density and Capacitance in TiO_2 Nanotube Arrays Induced by Electrochemical Doping," *J. Am. Chem. Soc.*, **130**, 11312–6 (2008).

[5]J. Park, H. S. Kim, and A. J. Bard, "Novel Carbon-Doped TiO_2 Nanotube Arrays with High Aspect Ratios for Efficient Solar Water Splitting," *Nano Lett.*, **6** [1] 248 (2006).

[6]I. Perez, E. Robertson, P. Banerjee, L. Henn-Lecordier, S. J. Son, S. B. Lee, and G. W. Rubloff, "TEM-Based Metrology for HfO_2 Layers and Nanotubes Formed in Anodic Aluminum Oxide Nanopore Structures," *Small*, **4** [8] 122332 (2008).

[7]S. A. Needham, G. X. Wang, H. K. Liu, and L. Yang, "Nickel Oxide Nanotubes: Synthesis and Electrochemical Performance for Use in Lithium Ion Batteries," *J. Nanosci. Nanotechnol.*, **6** [1] 7781 (2006).

[8]K. Hanabusa, T. Numazawa, S. Kobayashi, M. Suzuki, and H. Shirai, "Preparation of Metal Oxide Nanotubes Using Gelators as Structure-Directing Agents," *Macromol. Symp.*, **235**, 52–6 (2006).

[9]C. C. Tang, Y. Bando, B. D. Liu, and D. Golberg, "Cerium Oxide Nanotubes Prepared from Cerium Hydroxide Nanotubes,"*Adv. Mater.*, **17**, 30059 (2005).

[10]M. Kogiso, Y. Zhou, and T. Shimizu, "Instant Preparation of Self-Assembled Metal-Complexed Lipid Nanotubes that Act as Templates to Produce Metal Oxide Nanotubes," *Adv. Mater.*, **19**, 242–6 (2007).

[11]Y. Kobayashi, H. Hata, M. Salama, and T. E. Mallouk, "Scrolled Sheet Precursor Route to Niobium and Tantalum Oxide Nanotubes," *Nano Lett.*, **7** [7] 2142–5 (2007).

[12]S. Mukherjee, K. Kim, and S. Nair, "Short, Highly Ordered, Single-Walled Mixed-Oxide Nanotubes Assemble from Amorphous Nanoparticles," *J. Am. Chem. Soc.*, **129**, 6820–6 (2007).

[13]Y. Li, Y. Bando, and D. Golberg, "Single-Crystalline In_2O_3 Nanotubes Filled with in," *Adv. Mater.*, **15** [7–8] 581–5 (2003).

[14]V. V. Rajasekharan and D. A. Buttry, "Electrochemical Synthesis of Yttrium Oxide Nanotubes," *Chem. Mater.*, **18** [19] 4541–3 (2006).

[15]Y. Liu and M. Liu, "Growth of Aligned Square-Shaped SnO_2 Tube Arrays," *Adv. Funct. Mater.*, **15** [1] 57–62 (2005).

[16]M. M. Munir, H. Widiyandari, F. Iskandar, and K. Okuyama, "Patterned Indium Tin Oxide Nanofiber Films and Their Electrical and Optical Performance," *Nanotechnology*, **19**, 375601 (2008).

[17]Z. Y. Liu, D. Sun, P. Guo, and J. Q. Leckie, "An Efficient Bicomponent TiO_2/ SnO_2 Nanofiber Photocatalyst Fabricated by Electrospinning with a Side-by-Side Dual Spinneret Method," *Nano Lett.*, **7** [4] 1081–5 (2007).

[18]D. Li and Y. Xia, "Electrospinning of Nanofibers: Reinventing the Wheel," *Adv. Mater.*, **16** [14] 1151–70 (2004).

[19]Y. Wang and G. Cao, "Synthesis and Electrochemical Properties of $InVO_4$ Nanotube Arrays," *J. Mater. Chem.*, **17** [9] 894–9 (2007).

[20]L. Xu, L. Sang, C. Ma, Y. Lu, F. Wang, Q. Li, H. Dai, H. He, and J. Sun, "Preparation of Mesoporous $InVO_4$ Photocatalyst and its Photocatalytic Performance for Water Splitting," *Chinese J. Catal.*, **27** [2] 100–2 (2006).

[21]M. Touboul, K. Melghit, P. Bénard, and D. Louër, "Crystal Structure of a Metastable Form of Indium Orthovanadate, $InVO_4$-I," *J. Solid State Chem.*, **118**, 93–8 (1995).

[22]A. K. Alves, F. A. Berutti, F. J. Clemens, T. Graule, and C. P. Bergmann, "Photocatalytic Activity of Titania Fibers Obtained by Electrospinning," *Mater. Res. Bull.*, **44**, 312–7 (2009).

[23]G. Du, S. Feng, J. H. Zhao, C. Song, S. Bai, and Z. P. Zhu, "Particle-WireTube Mechanism for Carbon Nanotube Evolution," *J. Am. Chem. Soc.*, **128**, 15405–14 (2006).

[24]H. G. Liu, J. X. Yang, J. H. Liang, Y. X. Huang, and C. Y. Tangz, "ZnO Nanofiber and Nanoparticle Synthesized Through Electrospinning and Their Photocatalytic Activity Under Visible Light," *J. Am. Ceram. Soc.*, **91** [4] 1287–91 (2008).

[25]H. B. Zhang and M. J. Edirisinghe, "Electrospinning Zirconia Fiber from a Suspension," *J. Am. Ceram. Soc.*, **89** [6] 1870–5 (2006).

List of Figures

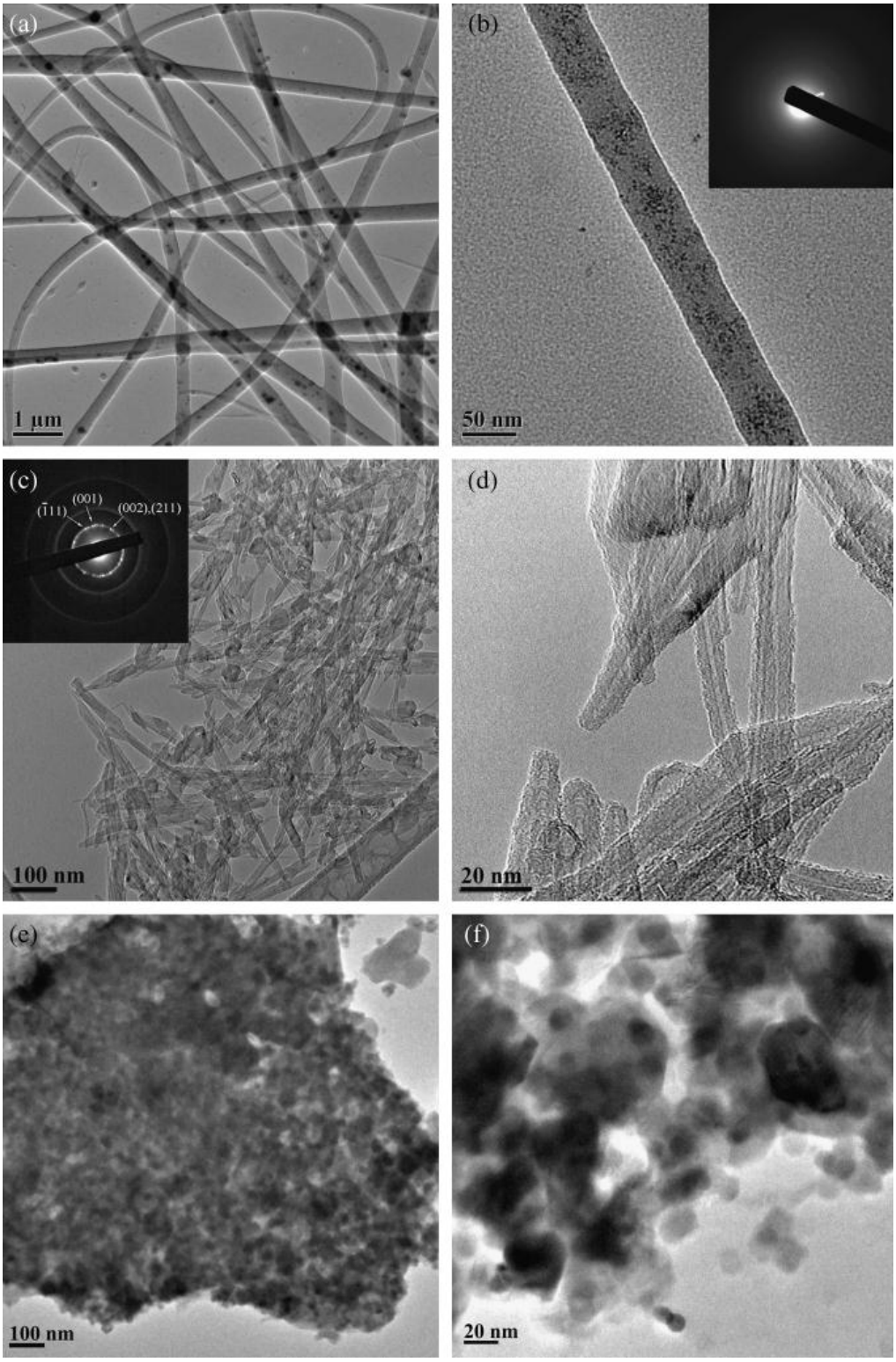

Fig. 1

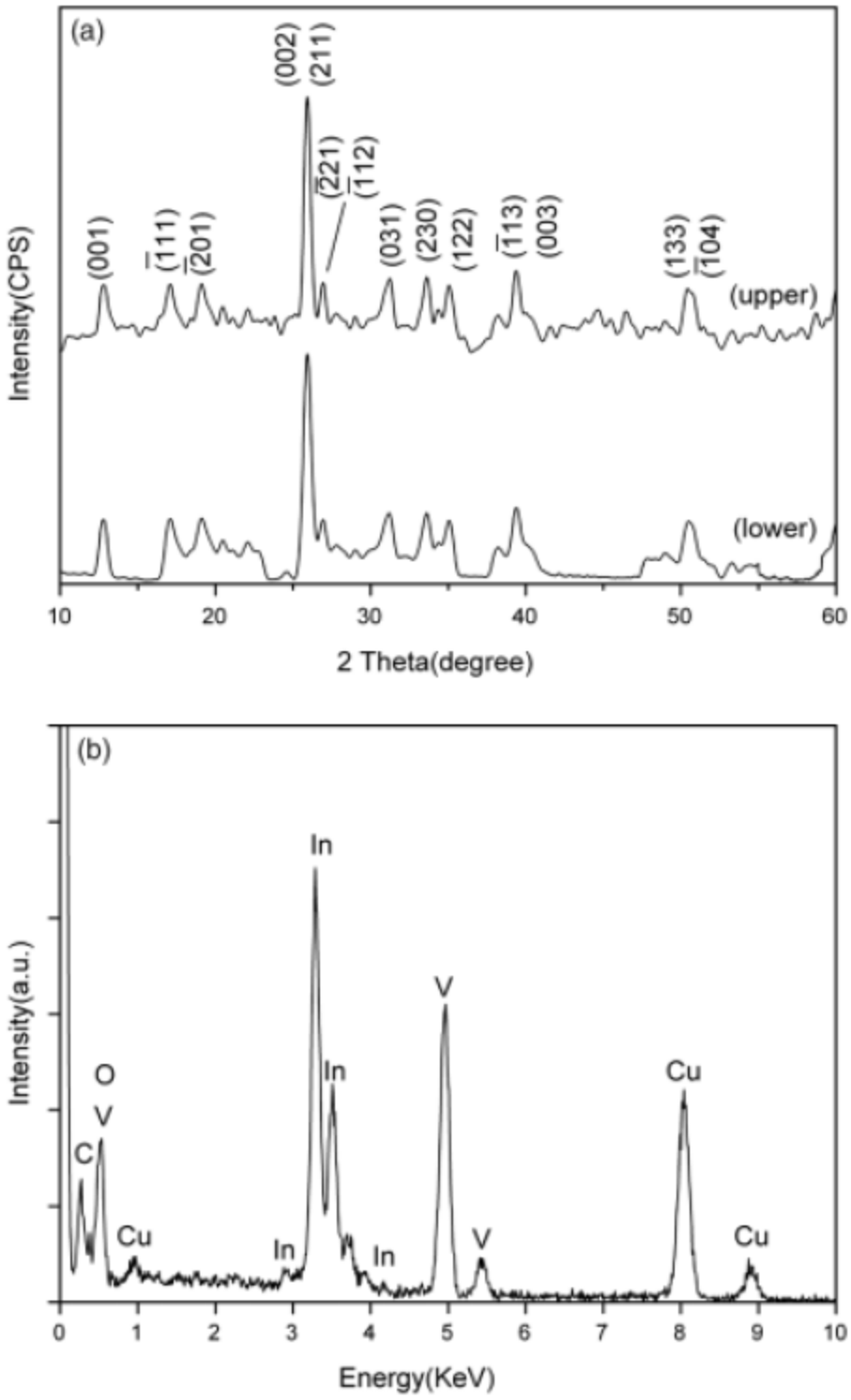
(a)
(002)
(211)
(001)
(111)
(201)
(221)
(112)
(031)
(230)
(122)
(113)
(003)
(133)
(104)
(upper)
(lower)
Intensity(CPS)
10
20
30
40
50
60
2 Theta(degree)
(b)
In
V
O
In
C
V
Cu
Cu
In
In
V
Cu
Intensity(a.u.)
0
1
2
3
4
5
6
7
8
9
10
Energy(KeV)

Fig. 2

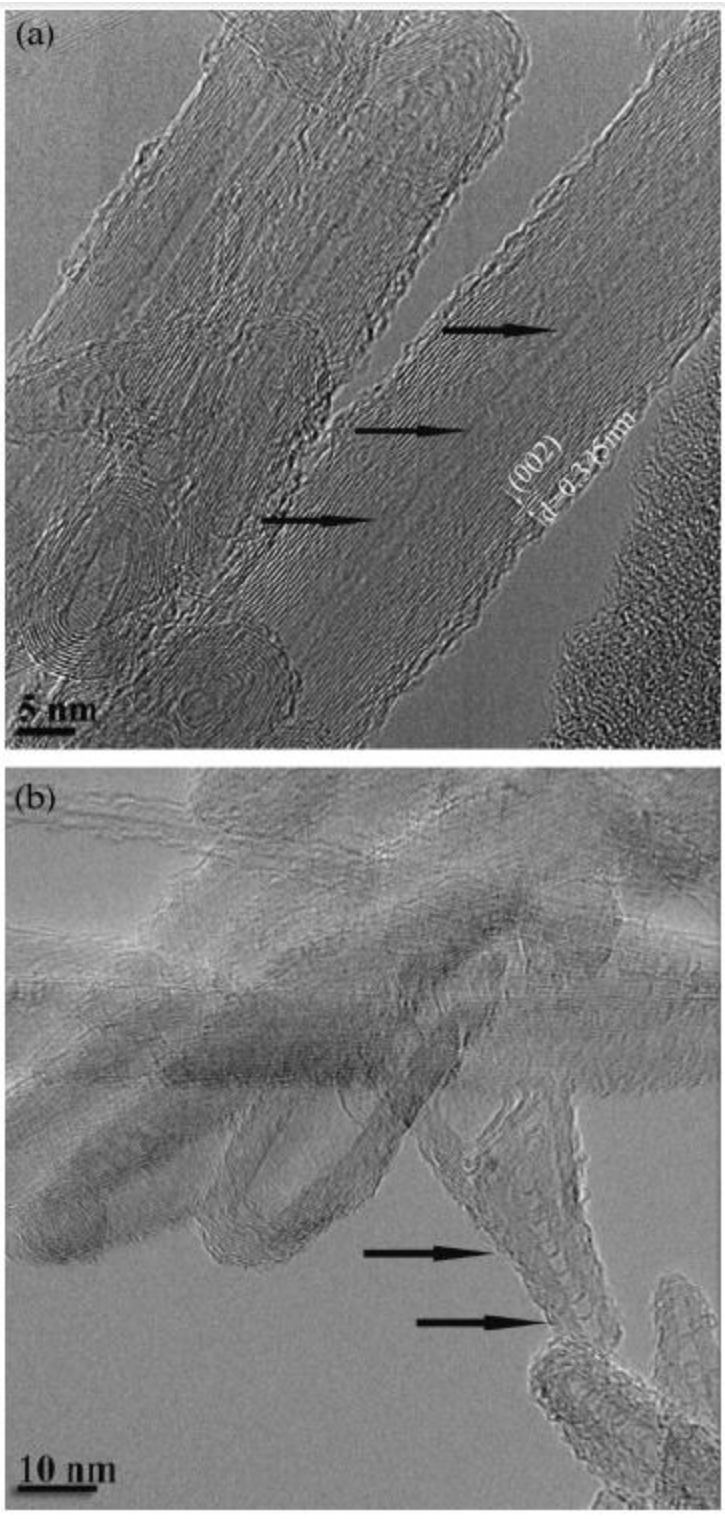

Fig. 3

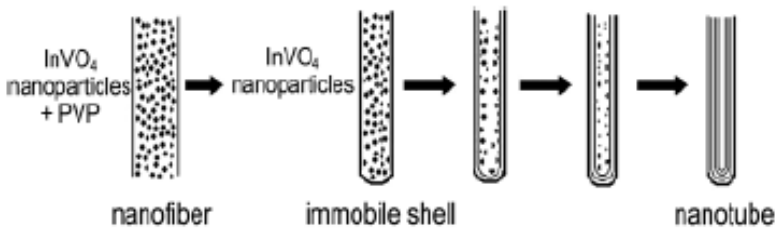
InVO4
nanoparticles
+ PVP
InVO4
nanoparticles
nanofiber
immobile shell
nanotube

Fig. 5